

ADDITIVE AVERAGE SCHWARZ METHOD FOR A CROUZEIX-RAVIART FINITE VOLUME ELEMENT DISCRETIZATION OF ELLIPTIC PROBLEMS WITH HETEROGENEOUS COEFFICIENTS

ATLE LONELAND, LESZEK MARCINKOWSKI, AND TALAL RAHMAN

ABSTRACT. In this paper we introduce an additive Schwarz method for a Crouzeix-Raviart Finite Volume Element (CRFVE) discretization of a second order elliptic problem with discontinuous coefficients, where the discontinuities are both inside the subdomains and across and along the subdomain boundaries. We show that, depending on the distribution of the coefficient in the model problem, the parameters describing the GMRES convergence rate of the proposed method depend linearly or quadratically on the mesh parameters H/h . Also, under certain restrictions on the distribution of the coefficient, the convergence of the GMRES method is independent of jumps in the coefficient.

1. INTRODUCTION

In this paper we introduce an additive Schwarz method for a second order elliptic problem with discontinuous coefficients inside the subdomains and across and along the subdomain boundaries. Problems of this type play a crucial part in the field of scientific computation. For example, simulation of fluid flow in porous media are often affected by discontinuities in the permeability of the porous media. Discontinuities or jumps in the coefficient cause the performance of standard iterative methods to deteriorate as the discontinuities or the jumps increase.

The finite volume (FV) method is one of the most versatile discretization techniques used in computational fluid dynamics. It is widely used for the approximation of conservation laws, nonlinear problems and in convection-diffusion problems. The finite volume divides the domain into control volumes where the nodes from the finite difference or the finite element discretization are located in the control volume. Unlike the finite difference and the finite element method, the solution to the finite volume method satisfies conservation of certain quantities such as mass, momentum, energy and species. This property is exactly satisfied for every control volume in the domain and also for the whole computational domain. An attractive feature of this method is that it is directly connected to the physics of the system. There are two types of finite volume methods: One which is based on the finite difference discretization, called the finite volume method and one which is based on the finite element discretization named the finite volume element (FVE) method. In the later the approximation of the solution is sought in a finite element space and can therefore be considered as a Petrov-Galerkin finite element method.

Due to the popularity of the finite volume element method in science and engineering, many results on the analysis of the FVE method have been published, cf. [21, 15, 25, 9, 10] and

Key words and phrases. domain decomposition, Crouzeix-Raviart element, additive Schwarz method, finite volume element, GMRES.

L. Marcinkowski was partially supported by the Polish Scientific Grant 2011/01/B/ST1/01179.

many more. In [1], the authors proved that for the Poisson equation on a polygonal domain in two dimension, the stiffness matrix of the FVE method is equal to the stiffness matrix of the FE method for very general grids. In [19], the authors proved that for the general elliptic case for polygonal domains in two dimensions, the error between the FE solution and the FVE solution is of first order in the general case and of second order for some special FVE schemes. Thus, some superconvergence results valid for the finite element method is also valid for the finite volume element method, cf. [8, 31]. Finite volume element methods based on the lowest order nonconforming Crouzeix-Raviart elements have been studied in [9], where the author proves optimal order error estimates in the L^2 -norm and a mesh dependent H^1 -norm for the FVE solution of elliptic problems. Later, the authors in [15] showed that the accuracy of the FVE method for linear conforming elements can be affected by the regularities of the exact solution and the source term. They also developed an error estimation framework for the FVE method which treats the FVE method as a perturbation of the Galerkin finite element method. For an overview over recent developments of FVE methods, cf. [21] and references therein.

Additive Schwarz Methods (ASM) for solving elliptic problems discretized by the finite element method have been studied thoroughly, cf. [28, 30], but ASMs for conforming finite volume element (FVE) discretization have only been consider in [11, 32]. For the CR finite element discretization, there exist several results for second order elliptic problems; cf. [27, 24, 3, 22], but for the CRFVE discretization, no ASMs have been studied.

In recent years, many results regarding ASMs for problems with discontinuities coefficient, both across and along subdomain boundaries, have been studied. In [18], the authors proposed a two level additive Schwarz method where the coarse space is based on the multiscale finite element functions introduced in [20]. Later, several authors have proposed two level additive Schwarz methods with coarse spaces based on spectral basis functions constructed from solving different types of generalized eigenvalue problems, cf. [16, 17, 12, 29] and many more. These method are all overlapping methods based on the conforming finite element discretization with exotic coarse spaces where the coarse basis functions are discrete harmonic functions or spectral basis functions.

The ASM we consider in this paper differs from methods mentioned above in the sense that it is a non-overlapping method and the discretization is done using nonconforming finite volume elements. Also, the average coarse space employed in our method is based on approximate discrete harmonic functions. Therefore, the average coarse space is a computationally cheap approximation to the full discrete harmonic function space. Also, the method does not require a coarse grid triangulation, i.e. we are free to use arbitrary irregular subdomains.

The variant of the additive Schwarz method we consider in this paper was first introduced for conforming P1 elements in [2] and later formulated for a mortar method with the Crouzeix-Raviart elements in [24]. In [13] the authors analyzed the method for a discontinuous Galerkin discretization. In this paper we consider the same additive Schwarz method for the Crouzeix-Raviart FVE method introduced in [9] and show that the method depends linearly or quadratically on the mesh parameters H/h , i.e., depending on the distribution of the coefficient in the model problem, the parameters describing the convergence of the GMRES method used to solve the preconditioned system depends linearly or quadratically on the mesh parameters. Under certain restrictions on the distribution of the coefficient, the convergence of the GMRES method is independent of jumps in the coefficient. Also, using the framework developed in [15], we prove the H^1 error estimates using the same techniques as in [15, 25]. This estimate is of optimal order if the exact solution of the elliptic problem

under consideration is of the H^2 regularity. Last, we show both theoretically and numerically that, in general, for varying coefficients the finite volume element bilinear form, and hence the resulting finite volume element stiffness matrix, is non-symmetric.

The rest of this paper is organized as follows. In Section 2 we define the differential problem and the discrete problem, both for the nonconforming finite element and the nonconforming finite volume element discretization. In Section 3 we introduce the GMRES method for the preconditioned system and the corresponding parameters describing the convergence rate. In Section 4 we introduce the additive Schwarz methods and give a detailed convergence analysis of the GMRES convergence rate. In Section 5 we show some numerical results which confirms the theory developed in the previous sections.

2. PRELIMINARIES

2.1. The Model Problem. We consider the following elliptic boundary value problem

$$(1) \quad \begin{aligned} -\nabla \cdot (\alpha(x) \nabla u) &= f && \text{in } \Omega, \\ u &= 0 && \text{on } \partial\Omega. \end{aligned}$$

Where Ω is a bounded convex domain in \mathbb{R}^2 and $f \in L^2(\Omega)$.

The corresponding standard variational (weak) formulation is: Find $u \in H_0^1(\Omega)$ such that

$$(2) \quad a(u, v) = \int_{\Omega} f v \, dx \quad \forall v \in H_0^1(\Omega),$$

where

$$a(u, v) = \int_{\Omega} \alpha(x) \nabla u \cdot \nabla v \, dx.$$

The coefficient $\alpha(x)$ has the property $\alpha \in W^{1,\infty}(D_j)$ with respect to a nonoverlapping partitioning of Ω into open, connected Lipschitz polytopes $\mathcal{D} := \{D_j : j = 1, \dots, n\}$, that is,

$$\bar{\Omega} = \bigcup_{j=1}^n \bar{D}_j.$$

We require that $|\alpha|_{1,\infty,D_j} \leq C$ for $j = 1, \dots, n$ and that $\alpha \geq \alpha_0$ for some positive constant α_0 . For simplicity of presentation we also require that $\alpha_0 \geq 1$. This last property can always be achieved by scaling of (1).

2.2. Basic notation. Throughout this paper we will use standard notations for the Sobolev spaces. We denote the space of functions that have weak derivatives of order s in the space $L^2(\Omega)$, as $H^s(\Omega)$. The norm on the space $H^s(\Omega)$ is defined by

$$\|u\|_{s,\Omega} = \|u\|_s = \left(\int_{\Omega} \sum_{|\alpha| \leq s} |D^\alpha u|^2 \, dx \right)^{1/2}.$$

The space of functions with bounded weak derivatives of order s is denoted by $W^{s,\infty}(\Omega)$ with the corresponding norm defined as

$$\|u\|_{s,\infty,\Omega} = \|u\|_{s,\infty} = \max_{0 \leq |\alpha| \leq s} \|D^\alpha u\|_2.$$

The subspace of $H^1(\Omega)$ with functions vanishing on the boundary $\partial\Omega$ in the sense of traces, is denoted by $H_0^1(\Omega)$. The duality pairing between $H^{-1}(\Omega)$ and $H_0^1(\Omega)$, denote by (f, u) is the action of a functional $f \in H^{-1}(\Omega)$ on a function $u \in H_0^1(\Omega)$.

Consider a triangulation \mathcal{T}_h of Ω , consisting of closed triangle elements K such that $\bar{\Omega} = \bigcup_{K \in \mathcal{T}_h} K$. Let h_K be the diameter of K and let $h = \max_{K \in \mathcal{T}_h} h_K$ be the largest diameter of the triangles $K \in \mathcal{T}_h$.

We assume that the triangulation is defined in such way that ∂K 's are aligned with ∂D_j 's. This implies that the coefficient $\alpha(x)$ has the property that $\alpha \in W^{1,\infty}(K)$ for all $K \in \mathcal{T}_h$. In addition, we also require the triangulation $\mathcal{T}_h(\Omega)$ to be quasiuniform [4].

We define the broken $H^1(\Omega)$ -norm and $H^1(\Omega)$ -seminorm respectively as

$$\|v\|_{s,h,\Omega} = \left(\sum_{K \in \mathcal{T}_h} \|v\|_{s,K}^2 \right)^{1/2} \quad \text{and} \quad |v|_{s,h,\Omega} = \left(\sum_{K \in \mathcal{T}_h} |v|_{s,K}^2 \right)^{1/2}.$$

We also introduce the energy seminorm

$$\|u\|_{a,G}^2 = \int_G \alpha(x) |\nabla u|^2 dx$$

for any $G \subset \Omega$ and let $\|u\|_a = \|u\|_{a,\Omega}$.

Let $E_h(K)$ be the set of edges of $K \in \mathcal{T}_h$ and $E_h = \bigcup_{K \in \mathcal{T}_h} E_h(K)$, i.e. the union of all edges in the triangulation \mathcal{T}_h . Also, define E_h^{in} as the set of interior edges of the triangulation \mathcal{T}_h , i.e. $e \in E_h^{\text{in}}$ if and only if $e \in E_h$ and $e \not\subset \partial\Omega$. For every edge $e \in E_h^{\text{in}}$ we identify a region V_e as the union of the two triangles K^{+e} and $K^{-e} \in \mathcal{T}_h$ sharing e as their common edge. Associated with this region, let $\mathcal{T}_h(V_e)$ be the set of the triangles of V_e and m_e the middle point of the edge $e \in E_h$ (cf. Figure 1).

Based on this triangulation \mathcal{T}_h , we introduce a dual mesh \mathcal{T}_h^* consisting of elements called the control volumes. There are several ways to construct the dual mesh. We choose here to construct the dual mesh in the following way. Let z_k be an interior point of $K \in \mathcal{T}_h$, we connect it with straight lines to the vertices of K such that K is partitioned into three subtriangles, K_e for each edge $e \in E_h(K)$. Denote this new finer triangulation of Ω by $\tilde{\mathcal{T}}_h$ and let, for every $K \in \mathcal{T}_h$, $\tilde{\mathcal{T}}_h(K) = \{\tilde{K} \in \tilde{\mathcal{T}}_h : \tilde{K} \text{ subtriangle of } K\}$ be the set of subtriangles of K .

We now associate with each edge $e \in E_h^{\text{in}}$ a corresponding control volume b_e consisting of the two subtriangles of $\tilde{\mathcal{T}}_h$ which have e as an common edge. Define $\mathcal{B}_e = \{b_e : e \in E_h^{\text{in}}\}$ to be the set of all such control volumes, and let n_e be the normal vector corresponding to the edge e in K^{+e} of the two triangles K^{+e} and K^{-e} sharing e .

We assume that there exists another nonoverlapping partitioning of Ω into open, connected Lipschitz polytopes Ω_i such that $\bar{\Omega} = \bigcup_{i=1}^N \bar{\Omega}_i$. We also assume that these subdomains form a coarse triangulation of the domain which is shape regular as in [5] and that the boundaries of elements in \mathcal{T}_h are aligned with the boundaries of any Ω_j .

For notational convenience, we denote the CR nodal points, i.e. the midpoints of edges $e \in E_h$, belonging to $\Omega, \Omega_i, \partial\Omega$ and $\partial\Omega_i$ by $\Omega_h^{\text{CR}}, \Omega_{ih}^{\text{CR}}, \partial\Omega_h^{\text{CR}}$ and $\partial\Omega_{ih}^{\text{CR}}$, respectively. Correspondingly, the set of P1 conforming nodal points, i.e., vertices of elements in $\mathcal{T}_h(\Omega)$ are denoted by $\Omega_h, \Omega_{ih}, \partial\Omega_h$ and $\partial\Omega_{ih}$, respectively. To simplify the presentation, we let C be a generic positive constant independent of the mesh sizes h and H , and of the functions under consideration. C may be different at different occurrences.

2.3. The CRFVE method. Let V_h be the nonconforming CR finite element space defined on the triangulation \mathcal{T}_h ,

$$V_h = V_h(\Omega) := \{v \in L^2(\Omega) : v|_K \in P_1, \quad K \in \mathcal{T}_h \quad v(m) = 0 \quad m \in \partial\Omega_h^{\text{CR}}\},$$

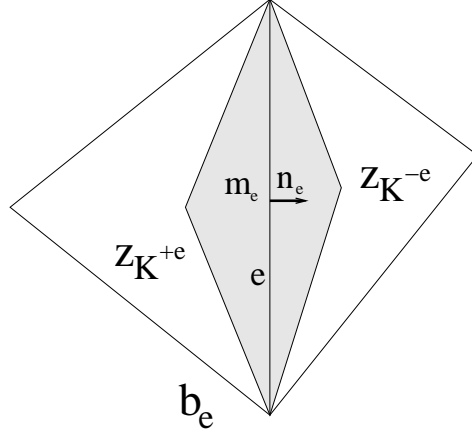


FIGURE 1. The control volume b_e for an edge e which is the common edge to the triangles K^{+e} and K^{-e} . Here m_e is the midpoint of e , n_e normal unit vector to e , $z_{K^{+e}}$ and $z_{K^{-e}}$ are the interior points of the triangles K^{+e} and K^{-e} which share the edge e .

and let V_h^* be its dual control volume space

$$V_h^* = V_h^*(\Omega) := \{v \in L^2(\Omega) : v|_{b_e} \in P_0, \quad b_e \in \mathcal{T}_h^* \quad v(m) = 0 \quad m \in \partial\Omega_h^{CR}\}.$$

Obviously, $V_h = \text{span}\{\phi_e(x) : e \in E_h\}$ and $V_h^* = \text{span}\{\chi_e(x) : e \in E_h\}$, where $\{\phi_e\}$ are the standard nonconforming nodal basis functions and $\{\chi_e\}$ are the characteristic functions of the control volume $\{b_e\}$. Now, we introduce two interpolation operators, I_h and I_h^* , defined for any function with properly defined and unique values at each midpoint $m \in \Omega_h^{CR}$, i.e.

$$I_h u = \sum_{e \in E_h^{in}} u(m_e) \phi_e \quad \text{and} \quad I_h^* u = \sum_{e \in E_h^{in}} u(m_e) \chi_e.$$

We may then define the CRFVE approximation u_h^{FV} of (1) as the solution to the following problem: Find $u_h^{FV} \in V_h$ such that

$$(3) \quad a_h^{FV}(u_h^{FV}, I_h^* v) = (f, I_h^* v), \quad v \in V_h$$

or equivalently

$$(4) \quad a_h^{FV}(u_h^{FV}, v) = (f, v), \quad v \in V_h^*,$$

where the bilinear form is defined as

$$(5) \quad a_h^{FV}(u, v) = - \sum_{e \in E_h^{in}} v(m_e) \int_{\partial b_e} \alpha(s) \nabla u \cdot \mathbf{n} \, ds \quad u \in V_h, v \in V_h^*.$$

The corresponding nonconforming finite element problem is defined as: Find $u_h^{FE} \in V_h$ such that

$$(6) \quad a_h^{FE}(u_h^{FE}, v) = (f, v), \quad v \in V_h,$$

where the CRFE bilinear form $a(\cdot, \cdot)$ is

$$(7) \quad a_h^{FE}(u, v) = \sum_{K \in T_h} \int_K \alpha(x) \nabla u \cdot \nabla v \, dx, \quad u, v \in V_h.$$

From the last bilinear form above we define a corresponding energy norm induced by $a_h^{FE}(\cdot, \cdot)$ as $\|\cdot\|_a = \sqrt{a_h^{FE}(\cdot, \cdot)}$.

Now we state a lemma which is needed to prove the relationship between the CRFVE- and CRFE-bilinear forms for piecewise constant coefficients $\alpha(x)$.

Lemma 2.1. *Let α be piecewise constant over each element, i.e., $\alpha_K = \alpha(x)|_K$ is constant for each $K \in \mathcal{T}_h(\Omega)$, $e \in E_h^{in} \cap E_h(K)$ and $v \in V_h$. Then*

$$(8) \quad \int_{b_e} \alpha(s) \frac{\partial u}{\partial n} ds = - \int_e \left[\frac{\partial u}{\partial n_e} \right]_\alpha ds.$$

where $\left[\frac{\partial u}{\partial n_e} \right]_\alpha = \alpha_{K^+e} \frac{\partial u}{\partial n_e} - \alpha_{K^-e} \frac{\partial u}{\partial n_e}$ and n_e is the normal vector of K to e .

Proof. Let $v \in V_h$, $K \in \mathcal{T}_h(\Omega)$, $e \in E_h^{in} \cap E_h(K)$ and n_e external normal vector of K to e . Then we have

$$\int_{\partial b_e} \alpha(s) \frac{\partial v}{\partial n} ds = \int_{\partial(b_e \cap K^+e)} \alpha_{K^+e} \frac{\partial v}{\partial n} ds + \int_{\partial(b_e \cap K^-e)} \alpha_{K^-e} \frac{\partial v}{\partial n} ds - \int_e \left[\frac{\partial v}{\partial n_e} \right]_\alpha ds.$$

Using Green's formula and the fact that $\Delta v = 0$ over $b_e \cap K^+e$ and $b_e \cap K^-e$ for any $e \in E_h^{in}$ we have

$$\int_{\partial(b_e \cap K^+e)} \frac{\partial v}{\partial n} ds = \int_{b_e \cap K^+e} \Delta v ds = 0,$$

and analogously for $\partial(b_e \cap K^-e)$. From this we obtain (8). \square

The next lemma is a classical result:

Lemma 2.2. *There exists a constant C independent of h such that*

$$C^{-1} |v|_{1,h}^2 \leq \sum_{K \in \mathcal{T}_h(\Omega)} \sum_{e,l \in E_h(K)} (v(m_e) - v(m_l))^2 \leq C |v|_{1,h}^2, \quad \forall v \in V_h.$$

The next lemma shows that if α is piecewise constant over fine elements then the CRFVE bilinear form is equal to the CRFE bilinear form, and in particular it is symmetric.

Lemma 2.3. *Let $u, v \in V_h$, and let α_K be piecewise constant over each element $K \in \mathcal{T}_h(\Omega)$, then*

$$(9) \quad a_h^{FE}(u, v) = a_h^{FV}(u, I_h^* v).$$

Proof. We express v as a linear combination of the basis elements of V_h , i.e. $v = \sum_{e \in E_h^{in}} v(m_e) \phi_e$. We may then write

$$(10) \quad \begin{aligned} a_h^{FE}(u, v) &= \sum_{K \in \mathcal{T}_h} \alpha_K \int_K \nabla u \cdot \nabla v dx \\ &= \sum_{e \in E_h^{in}} v(m_e) \sum_{K \in \mathcal{T}_h(V_e)} \alpha_K \int_K \nabla u \cdot \nabla \phi_e dx \end{aligned}$$

For each $e \in E_h^{in}$ and $u \in V_h$, we have

$$\begin{aligned}
\sum_{K \in \mathcal{T}_h(V_e)} \alpha_K \int_K \nabla u \cdot \nabla \phi_e \, dx &= \sum_{K \in \mathcal{T}_h(V_e)} \alpha_K \int_{\partial K} \frac{\partial u}{\partial n} \phi_e \, ds \\
&= \alpha_{K^+e} \int_{\partial K^+e} \frac{\partial u}{\partial n} \phi_e \, ds + \alpha_{K^-e} \int_{\partial K^-e} \frac{\partial u}{\partial n} \phi_e \, ds \\
&= \alpha_{K^+e} \int_{\partial K^+e \setminus e} \frac{\partial u}{\partial n} \phi_e \, ds + \alpha_{K^-e} \int_{\partial K^-e \setminus e} \frac{\partial u}{\partial n} \phi_e \, ds \\
&\quad + \alpha_{K^+e} \int_e \frac{\partial u}{\partial n_e} \phi_e \, ds - \alpha_{K^-e} \int_e \frac{\partial u}{\partial n_e} \phi_e \, ds
\end{aligned}$$

Using the fact that ϕ_e is a linear polynomial and $\frac{\partial u}{\partial n}$ is constant on every side of $K \in \mathcal{T}_h(V_e)$ we get

$$(11) \quad \sum_{K \in \mathcal{T}_h(V_e)} \alpha_K \int_K \nabla u \cdot \nabla \phi_e \, dx = \int_e \left[\frac{\partial u}{\partial n_e} \right]_\alpha \, ds,$$

Combining (10) and (11) we obtain

$$\begin{aligned}
a_h^{FE}(u, v) &= \sum_{e \in E_h^{in}} v(m_e) \int_e \left[\frac{\partial u}{\partial n_e} \right]_\alpha \, ds \\
(12) \quad &= - \sum_{e \in E_h^{in}} v(m_e) \int_{b_e} \alpha(s) \frac{\partial u}{\partial n} \, ds = a_h^{FV}(u, I_h^* v).
\end{aligned}$$

which completes the proof. \square

For varying coefficients in general, the FVE bilinear form is non-symmetric. This is easily seen by looking at $a_h^{FV}(\phi_i, I_h^* \phi_j)$ and $a_h^{FV}(\phi_j, I_h^* \phi_i)$. We state this as a remark.

Remark 2.4. For varying coefficients in (1), i.e. for a coefficient α which are not piecewise constant over each element, the FVE bilinear form is non-symmetric and hence in general we have

$$a_h^{FV}(\phi_i, I_h^* \phi_j) \neq a_h^{FV}(\phi_j, I_h^* \phi_i),$$

for two nodal basis functions $\phi_j, \phi_i \in V_h(\Omega)$.

Proof. Let i, j, l be the three indices for the edges of a triangle $K \in \mathcal{T}_h$, then we have for $a_h^{FV}(\phi_i, I_h^* \phi_j)$

$$\begin{aligned}
a_h^{FV}(\phi_i, I_h^* \phi_j) &= - \int_{\partial b_j} \alpha(s) \nabla \phi_i \cdot \mathbf{n} \, ds = - \int_{\partial(b_i \cap K) \cap \partial b_j} \alpha(s) \nabla \phi_i \cdot \mathbf{n} \, ds \\
(13) \quad &= - \nabla \phi_i \cdot \mathbf{n}_{jl} \int_{\partial(b_j \cap b_l)} \alpha(s) \, ds - \nabla \phi_i \cdot \mathbf{n}_{ji} \int_{\partial(b_j \cap b_i)} \alpha(s) \, ds
\end{aligned}$$

similarly for $a_h^{FV}(\phi_j, \phi_i)$ we have

$$\begin{aligned}
a_h^{FV}(\phi_j, I_h^* \phi_i) &= - \int_{\partial b_i} \alpha(s) \nabla \phi_j \cdot \mathbf{n} \, ds = - \int_{\partial(b_i \cap K) \cap \partial b_i} \alpha(s) \nabla \phi_j \cdot \mathbf{n} \, ds \\
(14) \quad &= - \nabla \phi_j \cdot \mathbf{n}_{il} \int_{\partial(b_i \cap b_l)} \alpha(s) \, ds - \nabla \phi_j \cdot \mathbf{n}_{ij} \int_{\partial(b_i \cap b_j)} \alpha(s) \, ds
\end{aligned}$$

where \mathbf{n}_{ij} , \mathbf{n}_{ji} , \mathbf{n}_{jl} and \mathbf{n}_{il} are the corresponding normal vectors w.r.t. the edges of the control volumes b_i , b_j and b_l corresponding to the edges $e_i, e_j, e_l \in E_h(K)$. Comparing the terms of (13) and (14) we see that in the last term of each equation the integral is over the same edge, but in the first term the integral of the coefficient is over different edges. Since α may be arbitrarily different at those edges, the first terms of (13) and (14) will also be arbitrarily different at thus in general we will have that

$$a_h^{FV}(\phi_i, I_h^* \phi_j) \neq a_h^{FV}(\phi_j, I_h^* \phi_i).$$

This completes the proof. \square

The next lemma is crucial for the analysis of our method. It relates the CRFVE and CRFE bilinear forms.

Lemma 2.5. *For the bilinear forms $a_h^{FE}(u, v)$ and $a_h^{FV}(u, v)$ the following estimates holds*

$$(15) \quad |a_h^{FE}(u, v) - a_h^{FV}(u, I_h^* v)| \leq Ch \|u\|_a \|v\|_a, \quad \forall u, v \in V_h.$$

and

$$(16) \quad a_h^{FV}(u, I_h^* u) \leq C_1 \|u\|_a \|v\|_a$$

$$(17) \quad a_h^{FV}(u, I_h^* u) \geq C_0 \|u\|_a^2$$

where C, C_0, C_1 are positive constants independent of h .

Proof. Similar results can be found in [25, 11] in the case of standard FVE method. For all $\alpha(x) \in W^{1,\infty}(K)$, define

$$\bar{\alpha}_K = \frac{1}{|K|} \int_K \alpha(x) dx, \quad K \in \mathcal{T}_h$$

and for all $u, v \in V_h$ define

$$\bar{a}(u, v) = \sum_{K \in \mathcal{T}_h} \int_K \bar{\alpha}_K \nabla u \cdot \nabla v dx,$$

and

$$\bar{a}_h(u, I_h^* v) = - \sum_{e \in \mathbb{E}_h^{in}} v(m_e) \int_{\partial b_e} \bar{\alpha}_K \nabla u \cdot \mathbf{n} ds.$$

Since $\bar{\alpha}_K$ is piecewise constant we have from Lemma 2.3

$$\bar{a}(u, v) = \bar{a}_h(u, I_h^* v),$$

which gives us

$$\begin{aligned} a_h^{FE}(u, v) - a_h^{FV}(u, I_h^* v) &= [a_h^{FE}(u, v) - \bar{a}(u, v)] + [\bar{a}_h(u, I_h^* v) - a_h^{FV}(u, I_h^* v)] \\ &= \text{I} + \text{II}. \end{aligned}$$

Since ∇u and ∇v are constant over each element K , we have

$$\text{I} = 0.$$

Write II as

$$\text{II} = \sum_{e \in \mathbb{E}_h^{in}} v(m_e) \int_{\partial b_e} (\alpha(s) - \bar{\alpha}_K) \nabla u \cdot \mathbf{n} ds$$

Define $\gamma_{el} = \partial b_e \cap \partial b_l$. The Cauchy-Schwarz inequality and Bramble-Hilbert give us

$$\begin{aligned}
|\text{II}| &= \left| \sum_{K \in \mathcal{T}_h} \sum_{e, l \in E_h(K)} (v(m_e) - v(m_l)) \int_{\gamma_{el}} (\alpha(s) - \bar{\alpha}_K) \nabla u \cdot \mathbf{n}_{\gamma_{el}} ds \right| \\
&\leq \sum_{K \in \mathcal{T}_h} \sum_{e, l \in E_h(K)} \|(\alpha(s) - \bar{\alpha}_K) \nabla u\|_{0, \infty, K} h_k |v(m_e) - v(m_l)| \\
&\leq C \left(\sum_{K \in \mathcal{T}_h} \sum_{e, l \in E_h(K)} \|(\alpha(s) - \bar{\alpha}_K) \nabla u\|_{0, \infty, K}^2 h_k^2 \right)^{1/2} \left(\sum_{K \in \mathcal{T}_h} \sum_{e, l \in E_h(K)} |v(m_e) - v(m_l)|^2 \right)^{1/2} \\
&\leq C \left(\sum_{K \in \mathcal{T}_h} C^2 h_K^2 |\alpha(s)|_{1, \infty, K}^2 \|\nabla u\|_{0, K}^2 \right)^{1/2} \left(\sum_{K \in \mathcal{T}_h} \sum_{e, l \in E_h(K)} |v(m_e) - v(m_l)|^2 \right)^{1/2} \\
&\leq Ch |u|_{1, h} |v|_{1, h} \leq Ch \|u\|_a \|v\|_a.
\end{aligned}$$

Above we have used the shape regular and quasi-uniform property of the triangulation and the fact that $\alpha \geq 1$ and $|\alpha(x)|_{1, \infty, K}$ is uniformly bounded over Ω . The estimates (16) and (17) then follow directly from (15), cf. [23] for details. \square

If we define for $u, v \in V_h$

$$(18) \quad a_h^{FV}(u, I_h^* v) = a_h^{FE}(u, v) + E_h(u, v)$$

then, in the the proof of Lemma 2.5, we see that there exists a constant independent of h , such that

$$(19) \quad E_h(u, v) \leq Ch \|u\|_{1, h} \|v\|_{1, h}.$$

For the CRFVE solution, u_h^{FV} , we also have

$$(20) \quad a_h^{FE}(u_h^{FV}, v) = (f, I_h^* v) - E_h(u_h^{FV}, v).$$

The lemma above and the resulting properties are crucial in the analysis of our additive Schwarz method. By applying them and using the framework developed in [15] we are able to prove the H^1 error estimates formulated in the following theorem:

Theorem 2.6. *For an exact solution $u \in H^{1+\beta}(\Omega)$ of (2), with $1/2 < \beta \leq 1$, $f \in L^2(\Omega)$, $\alpha(x) \in W^{1, \infty}(K)$ and for the CRFVE solution u_h^{FV} , we have*

$$(21) \quad \|u - u_h^{FV}\|_{1, h} \leq Ch^\beta (\|f\|_0 + \|u\|_{1+\beta}),$$

where the constant $C = C(\alpha)$ is independent of h .

Proof. A similar proof is given in [25, 15].

Let $I_h u \in V_h$ be the CRFE interpolant of u and let $I_h^* u \in V_h^*$ be the CRFVE interpolant of u . We start the proof by estimating $\|u_h^{FV} - I_h u\|_{1, h}$. From the coercivity property (17) we have

$$\begin{aligned}
C_0 \|u_h^{FV} - I_h u\|_{1,h}^2 &\leq a_h^{FV}(u_h^{FV} - I_h u, I_h^*(u_h^{FV} - I_h u)) \\
&= a_h^{FV}(u_h^{FV}, I_h^*(u_h^{FV} - I_h u)) - a_h^{FV}(I_h u, I_h^*(u_h^{FV} - I_h u)) \\
&= (f, I_h^*(u_h^{FV} - I_h u)) - a_h^{FE}(u_h^{FE}, u_h^{FV} - I_h u) \\
&\quad - a_h^{FE}(I_h u - u_h^{FE}, u_h^{FV} - I_h u) - E_h(I_h u, u_h^{FV} - I_h u).
\end{aligned}
\tag{22}$$

In the equations above we have used (20) and (18). For clarity of presentation we will split equation (22) into three parts and estimate each part independently. Using (6) and Lemma 5.1 in [10] the two first terms of (22) may be estimated by

$$\begin{aligned}
(f, I_h^*(u_h^{FV} - I_h u)) - a_h^{FE}(u_h^{FE}, u_h^{FV} - I_h u) &= (f, I_h^*(u_h^{FV} - I_h u) - (u_h^{FV} - I_h u)) \\
&\leq Ch \|f\|_0 \|u_h^{FV} - I_h u\|_{1,h}.
\end{aligned}$$

From approximation theory, cf. [4], we have that

$$\|u - I_h u\|_{1,h} \leq Ch^\beta \|u\|_{1+\beta} \tag{23}$$

$$\|I_h u\|_{1,h} \leq C \|u\|_{1+\beta} \tag{24}$$

which together with the continuity of the finite element bilinear form let us bound the second last remaining term by

$$\begin{aligned}
a_h^{FE}(I_h u - u_h^{FE}, u_h^{FV} - I_h u) &\leq C \|I_h u - u_h^{FE}\|_{1,h} \|u_h^{FV} - I_h u\|_{1,h} \\
&\leq C (\|I_h u - u\|_{1,h} + \|u - u_h^{FE}\|_{1,h}) \|u_h^{FV} - I_h u\|_{1,h} \\
&\leq Ch^\beta \|u\|_{1+\beta} \|u_h^{FV} - I_h u\|_{1,h}.
\end{aligned}$$

In the second line above we have used the finite element error estimate given below [4]

$$\|u - u_h^{FE}\|_{1,h} \leq Ch^\beta \|u\|_{1+\beta}.$$

The last term follows straightforwardly from (19)

$$\begin{aligned}
E_h(I_h u, u_h^{FV} - I_h u) &\leq Ch \|I_h u\|_{1,h} \|u_h^{FV} - I_h u\|_{1,h} \\
&\leq Ch \|u\|_{1+\beta} \|u_h^{FV} - I_h u\|_{1,h}.
\end{aligned}$$

Now, combining the estimates above with the results from approximation theory (23)–(24), we get

$$\begin{aligned}
\|u - u_h^{FV}\|_{1,h} &= \|u - I_h u - (u_h^{FV} - I_h u)\|_{1,h} \\
&\leq \|u - I_h u\|_{1,h} + \|u_h^{FV} - I_h u\|_{1,h} \\
&\leq Ch^\beta \|u\|_{1+\beta} + Ch^\beta (\|f\|_0 + \|u\|_{1+\beta}).
\end{aligned}
\tag{25}$$

This completes the proof. \square

The main idea in the above proof is motivated by [25, 15] which in turn was motivated by [9]. One of the advantage is that the estimate for $\|u_h^{FV} - I_h u\|_{1,h}$ is not needed, and the approach is more direct and simpler and allows us to apply standard CR finite element error estimation techniques.

3. THE GMRES METHOD

The linear system of equations which arises from problem (3) is in general non-symmetric. A popular method for solving such systems is the preconditioned GMRES method; cf. Saad and Schultz [26] and Eisenstat, Elman and Schultz [14]. This method has proven to be quite powerful for a large class of non-symmetric problems. The theory originally developed for $L^2(\Omega)$ in [14] can easily be extended to an arbitrary Hilbert space; cf. [6], see also [7].

We will in this paper use GMRES to solve the linear system of equations

$$(26) \quad Tu = g,$$

where T is a non-symmetric, nonsingular operator, $g \in V_h$ is the right hand side and $u \in V_h$ is the solution vector.

The core of the GMRES method is to solve a least square problem in each iteration, i.e. at step m we approximate the exact solution $u^* = T^{-1}g$ by a vector $u_m \in \mathcal{K}_m$ which minimizes the norm of the residual, where \mathcal{K}_m is the m -th Krylov subspace defined as

$$\mathcal{K}_m = \text{span} \{r_0, Tr_0, \dots, T^{m-1}r_0\}$$

and $r_0 = g - Tu_0$. In other words, z_m solves

$$\min_{z \in \mathcal{K}_m} \|g - T(u_0 + z)\|_a.$$

Hence, the m -th iterate is $u_m = u_0 + z_m$.

The convergence rate of the GMRES method is usually expressed in terms of the following two parameters

$$c_p = \inf_{u \neq 0} \frac{a(Tu, u)}{\|u\|_a^2} \text{ and } C_p = \sup_{u \neq 0} \frac{\|Tu\|_a}{\|u\|_a},$$

where c_p corresponds to the smallest eigenvalue of $\frac{1}{2}(T^t + T)$ the symmetric part of T and C_p corresponds to the square root of the largest eigenvalue of $T^t T$. Here T^t is the transpose of T with respect to the inner product $a(\cdot, \cdot)$.

The main results regarding the convergence of the GMRES method is stated in the next theorem. It describes the decrease of the norm of the residual in a single step.

Theorem 3.1 (Eisenstat-Elman-Schultz). *If $c_p > 0$, then the GMRES method converges and after m steps, the norm of the residual is bounded by*

$$(27) \quad \|r_m\|_a \leq \left(1 - \frac{c_p^2}{C_p^2}\right)^{m/2} \|r_0\|_a,$$

where $r_m = g - Tu_m$.

In the next section we will in Theorem 4.7 estimate the two parameters describing the convergence rate of the GMRES method once the proposed domain decomposition preconditioner corresponding to the operator T is defined and analyzed.

4. AN ADDITIVE AVERAGE METHOD

In this section we introduce the additive method for the discrete problem (3) and provide bounds on the convergence rate, both for the solution of the symmetric and non-symmetric problem.

4.1. Decomposition of $V_h(\Omega)$. We decompose the original space into

$$(28) \quad V_h(\Omega) = V_0(\Omega) + V_1(\Omega) + \cdots + V_N(\Omega),$$

where for $i = 1, \dots, N$ we have defined $V_i(\Omega)$ as the restriction of $V_h(\Omega)$ to Ω_i with functions vanishing on $\partial\Omega_{ih}^{CR}$ and as well as on the other subdomains. The coarse space $V_0(\Omega)$ is defined as the range of the interpolation operator I_A . For $u \in V_h(\Omega)$, we let $I_A u \in V_h(\Omega)$ be defined as

$$(29) \quad I_A u := \begin{cases} u(x), & x \in \partial\Omega_{ih}^{CR} \\ \hat{u}_i, & x \in \Omega_{ih}^{CR} \end{cases}$$

where

$$(30) \quad \hat{u}_i := \frac{1}{n_i} \sum_{x \in \partial\Omega_{ih}^{CR}} u(x).$$

Here n_i is the number of nodal points of $\partial\Omega_{ih}^{CR}$.

We also assume that $\mathcal{T}_h(\Omega_i)$ inherits the shape regular and quasi-uniform triangulation for each Ω_i with mesh parameters h_i and $H_i = \text{diam}(\Omega_i)$. The layer along $\partial\Omega_i$ consisting of unions of triangles $K \in \mathcal{T}(\Omega_i)$ which touch $\partial\Omega_i$ is denoted as Ω_i^δ .

The local bilinear form is chosen as the CRFE symmetric bilinear form $a_h^{FE}(u, v)$ or as the non-symmetric CRFVE bilinear form $a_h^{FV}(u, v)$.

For $i = 0, \dots, N$ we define the projection like operators $T_i: V_h \rightarrow V_i$ as

$$(31) \quad a_h^{FE}(T_i^{(1)} u, v) = a_h^{FE}(u, v) \quad \forall v \in V_i(\Omega),$$

for the symmetric problem (6). For the non-symmetric problem (3) we introduce two similar projection like operators. The first one which is symmetric is defined as

$$(32) \quad a_h^{FE}(T_i^{(2)} u, v) = a_h^{FV}(u, I_h^* v) \quad \forall v \in V_i(\Omega),$$

and the second one which is non-symmetric is defined as

$$(33) \quad a_h^{FV}(T_i^{(3)} u, v) = a_h^{FV}(u, I_h^* v) \quad \forall v \in V_i(\Omega).$$

Each of these problems have a unique solution. We now introduce

$$(34) \quad T_A^{(k)} := T_0^{(k)} + T_1^{(k)} + \cdots + T_N^{(k)}, \quad k = 1, 2, 3$$

which allow us to replace the original problem (3) for $k = 1$ or (6) for $k = 2, 3$ by the equation

$$(35) \quad T_A^{(k)} u = g^{(k)},$$

where $g^{(k)} = \sum_{i=0}^N g_i$ and $g_i^{(k)} = T_i^{(k)} u$. Note that $g_i^{(k)}$ may be computed without knowing the solution u of (3) or (6), respectively.

4.2. Analysis. Let $V_h^{quad}(\Omega_i)$ be the space of continuous piecewise quadratic functions on $T_h(\Omega_i)$. We introduce a local equivalence mapping $\mathcal{M}_i: V_h(\Omega_i) \rightarrow V_h^{quad}(\Omega_i)$ in a similar way as in [3]. Let m_x be an adjacent midpoint of a vertex x if both points belong to the same edge in $T_h(\Omega_i)$. The choice of the midpoint is not unique and this fact will be used below. Note that the degrees of freedom of $V_h^{quad}(\Omega_i)$ is the sum of $\bar{\Omega}_{ih}^{CR}$ and $x \in \bar{\Omega}_{ih}$.

Definition 4.1. For $u \in V_h(\Omega_i)$,

$$(36) \quad \mathcal{M}_i u(m) = \begin{cases} u(m), & m \in \bar{\Omega}_{ih}^{CR}, \\ u(m_x) & x \in \bar{\Omega}_{ih} \end{cases}$$

The properties of such equivalence mapping, which we are going to use later, are given in the following lemma.

Lemma 4.2. Let $\mathcal{M}_i : V_h(\Omega_i) \rightarrow V_h^{quad}(\Omega_i)$ be the local equivalence mapping defined above. The adjacent midpoint m_x is picked as the one whose distant to $\partial\Omega_i$ is the smallest, in particular if $x \in \partial\Omega_{ih}$ then the adjacent midpoint is in $\partial\Omega_{ih}^{CR}$.

Then, for any $u \in V_h(\Omega_i)$ we have

$$(37) \quad |u|_{1,h,\Omega_i} \leq |\mathcal{M}_i u|_{1,\Omega_i} \leq C |u|_{1,h,\Omega_i},$$

$$(38) \quad \|u - \mathcal{M}_i u\|_{0,\Omega_i} \leq Ch |u|_{1,h,\Omega_i},$$

$$(39) \quad |\mathcal{M}_i u|_{1,\partial\Omega_i}^2 \leq Ch_i^{-1} |u|_{1,h,\Omega_i^\delta}^2$$

Here Ω_i^δ is the sum of all triangles $K \in T_h(\Omega_i)$ such that K has an edge or a vertex on $\partial\Omega_i$.

Proof. The first two statements can be proven in the same way as in [3].

We will prove the last one only.

$$|\mathcal{M}_i u|_{1,\partial\Omega_i}^2 = \sum_{e \in E_h(\partial\Omega_i)} |\mathcal{M}_i u|_{1,e}^2 \leq C \sum_{e \in E_h(\partial\Omega_i)} \sum_{x \in \partial e} \frac{1}{|e|} |\mathcal{M}_i u(x) - \mathcal{M}_i u(m_e)|^2$$

where $m_e \in \partial\Omega_{ih}^{CR}$ is the midpoint of an edge e .

Note that by the definition of $\mathcal{M}_i u$ we get that $\mathcal{M}_i u(x) = \mathcal{M}_i u(m_x)$ where m_x is the adjacent midpoint in $\partial\Omega_{ih}^{CR}$, i.e. its left or right neighbor point.

Thus by the quasiuniformity of the triangulation and the definition of the equivalence mapping we get

$$|\mathcal{M}_i u|_{1,\partial\Omega_i}^2 \leq \frac{1}{h_i} \sum_{m,s \in \partial\Omega_{ih}^{CR}} |\mathcal{M}_i u(m) - \mathcal{M}_i u(s)|^2 = \frac{1}{h_i} \sum_{m,s \in \partial\Omega_{ih}^{CR}} |u(m) - u(s)|^2$$

where m and s are neighboring CR points on $\partial\Omega_i$. Let $x \in \partial\Omega_{ih}$ denote the vertex lying between them, and let $\{m_{x,k}\} \subset \Omega_{k,h}^{CR}$ be adjacent midpoints numbered in such a way that two successive ones are in one closed element. Then from the shape regularity of the triangulation the number of those midpoints is bounded and a triangle inequality yields that

$$|u(m) - u(s)| \leq |u(m) - u(m_1)| + |u(m_1) - u(m_2)| \dots + |u(m_k) - u(s)|$$

Thus, using this and Lemma 2.2 yields that

$$|u(m) - u(s)|^2 \leq C \sum_{x \in \partial K} |u|_{H^1(K)}^2.$$

where the sum is taken over all elements K in Ω_k which has x as a vertex.

Summing the above estimates over all edges yields the following bound:

$$|\mathcal{M}_i u|_{1,\partial\Omega_i}^2 \leq Ch_i^{-1} |u|_{1,h,\Omega_i^\delta}^2.$$

□

We are now ready to prove two lemmas for the interpolation-like operator I_A which will help us analyze and prove the main theorems of our proposed method.

Lemma 4.3. *For any $u \in V_h$ the following holds:*

$$(40) \quad a_h^{FE}(I_A u, I_A u) \leq C \max_i \left(\frac{\bar{\alpha}_i H_i^2}{\underline{\alpha}_i h_i^2} \right) a_h^{FE}(u, u),$$

where $\bar{\alpha}_i := \sup_{x \in \bar{\Omega}_i^\delta} \alpha(x)$, $\underline{\alpha}_i := \inf_{x \in \bar{\Omega}_i^\delta} \alpha(x)$ and C is a positive constant independent of $\alpha, \frac{\bar{\alpha}_i}{\underline{\alpha}_i}, H_i$ and h_i .

Proof. The idea behind the proof comes from [13]. We start the proof by estimating

$$\begin{aligned} \|I_A u\|_{a, \Omega_i}^2 &= \|I_A u\|_{a, \Omega_i^\delta}^2 \\ &\leq \bar{\alpha}_i |I_A u|_{1, h, \Omega_i^\delta}^2 \\ &\leq C \bar{\alpha}_i \sum_{K \in \mathcal{T}_h(\Omega_i^\delta)} \sum_{e, l \in \mathbb{E}_h(K)} (I_A u)(m_e) - (I_A u)(m_l))^2 \\ &\leq C \bar{\alpha}_i \sum_{x \in \partial \Omega_{ih}^{CR}} (u(x) - \hat{u}_i)^2 \\ &= C \bar{\alpha}_i \sum_{x \in \partial \Omega_{ih}^{CR}} (\mathcal{M}_i u(x) - \widehat{\mathcal{M}_i u})^2 \\ &\leq C \frac{\bar{\alpha}_i}{h_i} \|\mathcal{M}_i u - \widehat{\mathcal{M}_i u}\|_{0, \partial \Omega_i}^2, \end{aligned}$$

Applying the the Poincare inequality and (39) of Lemma 4.2 we may write

$$\begin{aligned} C \frac{\bar{\alpha}_i}{h_i} \|\mathcal{M}_i u - \widehat{\mathcal{M}_i u}\|_{0, \partial \Omega_i}^2 &\leq C \bar{\alpha}_i \frac{H_i^2}{h_i} |\mathcal{M}_i u|_{1, \partial \Omega_i}^2 \\ &\leq C \left(\frac{\bar{\alpha}_i H_i^2}{\underline{\alpha}_i h_i^2} \right) |u|_{1, h, \Omega_i^\delta}^2 \\ &\leq C \left(\frac{\bar{\alpha}_i H_i^2}{\underline{\alpha}_i h_i^2} \right) \|u\|_{a, \Omega_i^\delta}^2. \end{aligned}$$

Summing over all the subdomains and introducing $\max_i \left(\frac{\bar{\alpha}_i H_i^2}{\underline{\alpha}_i h_i^2} \right)$ we prove (40). \square

Under certain assumptions on the lower bound of $\alpha(x)$ in the interior of each Ω_i we may improve the above estimate with respect to $\frac{H_i}{h_i}$.

Lemma 4.4. *Let $\underline{\alpha}_i \leq \alpha(x)$ in $\Omega_i \setminus \Omega_i^\delta$. For any $u \in V_h$ the following holds:*

$$(41) \quad a_h^{FE}(I_A u, I_A u) \leq C \max_i \left(\frac{\bar{\alpha}_i H_i}{\underline{\alpha}_i h_i} \right) a_h^{FE}(u, u),$$

where $\bar{\alpha}_i := \sup_{x \in \bar{\Omega}_i^\delta} \alpha(x)$, $\underline{\alpha}_i := \inf_{x \in \bar{\Omega}_i^\delta} \alpha(x)$ and C is a positive constant independent of $\alpha, \frac{\bar{\alpha}_i}{\underline{\alpha}_i}, H_i$ and h_i .

Proof. From the proof of Lemma 4.3 we have that

$$\|I_A u\|_{a, \Omega_i}^2 \leq C \frac{\bar{\alpha}_i}{h_i} \|\mathcal{M}_i u - \widehat{\mathcal{M}_i u}\|_{0, \partial \Omega_i}^2.$$

Using a scaling argument and a trace theorem we may write:

$$\begin{aligned}
\|I_A u\|_{a,\Omega_i}^2 &\leq C \frac{\bar{\alpha}_i}{h_i} \|\mathcal{M}_i u - \widehat{\mathcal{M}_i u}\|_{0,\partial\Omega_i}^2 \\
(42) \quad &\leq C \bar{\alpha}_i \frac{H_i}{h_i} \left\{ |\mathcal{M}_i u|_{1,h,\Omega_i}^2 + H_i^{-2} \|\mathcal{M}_i u - \widehat{\mathcal{M}_i u}\|_{0,\partial\Omega_i}^2 \right\} \\
&\leq C \bar{\alpha}_i \frac{H_i}{h_i} |\mathcal{M}_i u|_{1,h,\Omega_i}^2 \\
&= C \bar{\alpha}_i \frac{H_i}{h_i} |u|_{1,h,\Omega_i}^2 \\
&\leq C \frac{\bar{\alpha}_i}{\underline{\alpha}_i} \frac{H_i}{h_i} \|u\|_{a,\Omega_i}^2
\end{aligned}$$

where we have used the properties of \mathcal{M}_i , and Poincaré's inequality on the last term in the curly brackets. Summing over all the subdomains and introducing $\max_i \left(\frac{\bar{\alpha}_i}{\underline{\alpha}_i} \frac{H_i}{h_i} \right)$ completes the proof. \square

Using the two lemmas above we may now state two theorems and two propositions for the convergence rate of our proposed preconditioner applied to the linear system arising from the symmetric problem (6) and for the linear system arising from the non-symmetric problem (3). We first prove the convergence rate for our ASM applied to the symmetric problem (6)

Theorem 4.5. *For any $u \in V_h$ the following holds:*

$$(43) \quad C_1 \beta_1^{-1} a_h^{FE}(u, u) \leq a_h^{FE}(T_A^{(1)} u, u) \leq C_2 a_h^{FE}(u, u),$$

where $\beta_1 = \max_i \left(\frac{\bar{\alpha}_i}{\underline{\alpha}_i} \frac{H_i^2}{h_i^2} \right)$ and the positive constants C_1 and C_2 is independent of $\alpha, \frac{\bar{\alpha}_i}{\underline{\alpha}_i}, H_i$ and h_i for $i = 1, \dots, N$.

Proof. Following the general theory of ASMs, we need to check the three key assumptions ([28, 30]).

Assumption (1). *For all $u \in V_h$ there exists a representation $u = \sum_{i=0}^N u_i$, $u_i \in V_i$, such that*

$$(44) \quad \sum_{i=0}^N a_h^{FE}(u_i, u_i) \leq C \beta_1 a_h^{FE}(u, u).$$

Let $u_0 = I_A u$ for $u \in V_h(\Omega)$ and $u_i := u - u_0$ on $\bar{\Omega}_i$ and $u_i = 0$ outside of Ω_i . Obviously $u_i \in V_i(\Omega)$ for $i = 0, \dots, N$, and $u = \sum_{i=0}^N u_i$. We then have

$$\begin{aligned}
\sum_{i=1}^N a_h^{FE}(u_i, u_i) + a_h^{FE}(u_0, u_0) &= \sum_{i=1}^N a_h^{FE}(u - u_0, u - u_0) + a_h^{FE}(u_0, u_0) \\
&\leq 2 \sum_{i=1}^N \{a_h^{FE}(u, u) + a_h^{FE}(u_0, u_0)\} + a_h^{FE}(u_0, u_0) \\
(45) \quad &= 2a_h^{FE}(u, u) + 3a_h^{FE}(u_0, u_0).
\end{aligned}$$

Using Lemma 4.3 on the last term we obtain β_1 in (44) immediately.

Assumption (2). Let $0 \leq \mathcal{E}_{ij} \leq 1$ be the minimal values that satisfy

$$a_h^{FE}(u_i, u_j) \leq \mathcal{E}_{ij} a_h^{FE}(u_i, u_i)^{1/2} a_h^{FE}(u_j, u_j)^{1/2}, \quad \forall u_i \in V, \forall u_j \in V_j, i, j = 1, \dots, N$$

Define $\rho(\mathcal{E})$ to be the spectral radius of $\mathcal{E} = \{\mathcal{E}_{ij}\}$.

In our case V_i and V_j are orthogonal for $i \neq j$, thus $\rho(\mathcal{E}) = 1$.

Since we are using exact bilinear forms the next assumption is trivially satisfied with $\omega = 1$ for $i = 1, \dots, N$.

Assumption (3). Let $\omega > 0$ be the minimal constant such that

$$a_h^{FE}(u, u) \leq \omega a_h^{FE}(u, u), \quad u \in V_i.$$

□

This results may be improved if the condition on the distribution of α in Lemma 4.4 is satisfied as shown in the next Proposition.

Proposition 4.6. Let $\underline{\alpha}_i \leq \alpha(x)$ in $\Omega_i \setminus \Omega_i^\delta$. For any $u \in V_h$ the following holds:

$$(46) \quad C_1 \beta_1^{-1} a_h^{FE}(u, u) \leq a(T_A^{(1)} u, u) \leq C_2 a_h^{FE}(u, u),$$

where $\beta_1 = \max_i \left(\frac{\overline{\alpha}_i H_i}{\underline{\alpha}_i h_i} \right)$ and the positive constants C_1 and C_2 is independent of $\alpha, \frac{\overline{\alpha}_i}{\underline{\alpha}_i}, H_i$ and h_i for $i = 1, \dots, N$.

Proof. The proof is completely analogous to Theorem 4.5, but Lemma 4.4 is applied instead of Lemma 4.3. □

The main theorem for the GMRES convergence rate of our ASM applied to the non-symmetric problem (3) is stated below

Theorem 4.7. There exists $h_0 > 0$ such that for all $h < h_0$, $k = 2, 3$, and $u \in V_h$, we have

$$\begin{aligned} \|T^{(k)} u\|_a &\leq C \|u\|_a, \\ a_h^{FE}(T^{(k)} u, u) &\geq c \max_i \frac{\overline{\alpha}_i}{\underline{\alpha}_i} \left(\frac{H_i}{h_i} \right)^{-2} a_h^{FE}(u, u), \end{aligned}$$

where C, c are positive constants independent of $\alpha, \frac{\overline{\alpha}_i}{\underline{\alpha}_i}, h_i$ and H_i for $i = 1, \dots, N$.

Proof. Following the framework of [23] we need to prove three assumptions.

Assumption (1). For all $u, v \in V_h$ the following holds

$$(47) \quad |a_h^{FE}(u, v) - a_h^{FV}(u, I_h^* v)| \leq Ch \|u\|_a \|v\|_a,$$

Assumption (2). For all $u \in V_h$ there exists a representation $u = \sum_{i=0}^N u_i$, $u_i \in V_i$, such that

$$(48) \quad \sum_{i=0}^N a_h^{FE}(u_i, u_i) \leq C \beta_1 a_h^{FE}(u, u).$$

Assumption (3). Let $0 \leq \mathcal{E}_{ij} \leq 1$ be the minimal values that satisfy

$$a_h^{FE}(u_i, u_j) \leq \mathcal{E}_{ij} a_h^{FE}(u_i, u_i)^{1/2} a_h^{FE}(u_j, u_j)^{1/2}, \quad \forall u_i \in V, \forall u_j \in V_j, i, j = 1, \dots, N$$

Define $\rho(\mathcal{E})$ to be the spectral radius of $\mathcal{E} = \{\mathcal{E}_{ij}\}$.

These assumptions have been proven in Theorem 4.5 and Lemma 2.5. \square

In the same way as for the convergence rate of our ASM applied to the symmetric problem we may improve the estimate of the last theorem if the condition of the distribution of α in Lemma 4.4 are satisfied.

Proposition 4.8. *There exists $h_0 > 0$ such that for all $h < h_0$, $k = 2, 3$, $u \in V_h$ and $\underline{\alpha}_i \leq \alpha(x)$ in $\Omega_i \setminus \Omega_i^\delta$, we have*

$$\begin{aligned} \|T^{(k)}u\|_a &\leq C\|u\|_a, \\ a_h^{FE}(T^{(k)}u, u) &\geq c \max_i \frac{\bar{\alpha}_i}{\underline{\alpha}_i} \left(\frac{H_i}{h_i}\right)^{-1} a_h^{FE}(u, u) \quad \forall u \in V_h, \end{aligned}$$

where C, c are positive constants independent of α , $\frac{\bar{\alpha}_i}{\underline{\alpha}_i}$, h_i and H_i for $i = 1, \dots, N$.

Proof. The proof is completely analogous to Theorem 4.7. The only difference is that the assumptions here have been proven in Lemma 2.5 and Proposition 4.6 instead of in Theorem 4.5. \square

5. NUMERICAL RESULTS

In this section we present some numerical results using the proposed method. All experiments are done for the Problem (1) on a unit square domain $\Omega = (0, 1)^2$. The coefficient α is equal to $2 + \sin(100\pi x) \sin(100\pi y)$ except for the areas marked with red where α equals $\alpha_1(2 + \sin(100\pi x) \sin(100\pi y))$ and α_1 is a parameter describing the discontinuities in the distribution of the coefficient. The right hand side is chosen to be $f = 1$.

The numerical solution is obtained by solving the preconditioned system (35) for k equal 2 using the generalized minimal residual method (GMRES). We run the method until the l_2 norm of the residual is reduced by a factor 10^6 , i.e., when $\|r_i\|_2 / \|r_0\|_2 \leq 10^{-6}$, r_i being the i -th residual.

In the first four examples we subdivide Ω into 4×4 subdomains and test the method for various distributions of the coefficient α . For example 1, we consider a distribution of α consisting of channels and inclusions in the interior of the subdomains, i.e. α has jumps only in the interior of subdomains (cf. Figure 2a). For Example 2 and 4, we consider distributions where α has jumps along subdomain interfaces (cf. Figure 2b and 3b) and therefore jumps also on the subdomain layers. In Example 3, we consider the case where α has jumps over substructures. For each of the examples above, the number of iterations until convergence for different values of α_1 , are shown in Table 3.

In Table 4 and 5 we report the iteration number for decreasing values of H_i and h_i for two test cases where the coefficient α is equal to $2 + \sin(10\pi x) \sin(10\pi y)$ and $2 + \sin(100\pi x) \sin(100\pi y)$, respectively. In the parentheses we report an estimate of the smallest eigenvalue of the symmetric part of the preconditioned operator $T_A^{(2)}$, i.e., the smallest eigenvalue of $\frac{1}{2} (T_A^{(2)t} + T_A^{(2)})$, which corresponds to the parameter c_p in Theorem 3.1.

In Table 6, we report the iteration number and estimate of the smallest eigenvalue for the symmetric part of the non-symmetric preconditioner for decreasing values of H_i and h_i , i.e., for k equal 3. The distribution of α is here the same as for the problem in Table 5.

We do not report any estimates of the parameter C_p of Theorem 3.1, which is defined as the square root of the largest eigenvalue of the normal matrix, $T_A^{(2)t} T_A^{(2)}$, since both our

convergence analysis and numerical results show that this is a constant independent of the coefficient α and the mesh parameters.

The magnitude of the non-symmetry and non-normality of the CRFVE stiffness matrix A with respect to α_1 are shown in Table 1 and the distributions of the eigenvalues of stiffness matrix A and the corresponding preconditioned operator, $T_A^{(2)}$, are shown in Figure 4 and 5, respectively. The difference between the finite element and the finite volume element stiffness matrices measured in the matrix 2-norm is shown in Table 2, for three different distributions of the coefficient α .

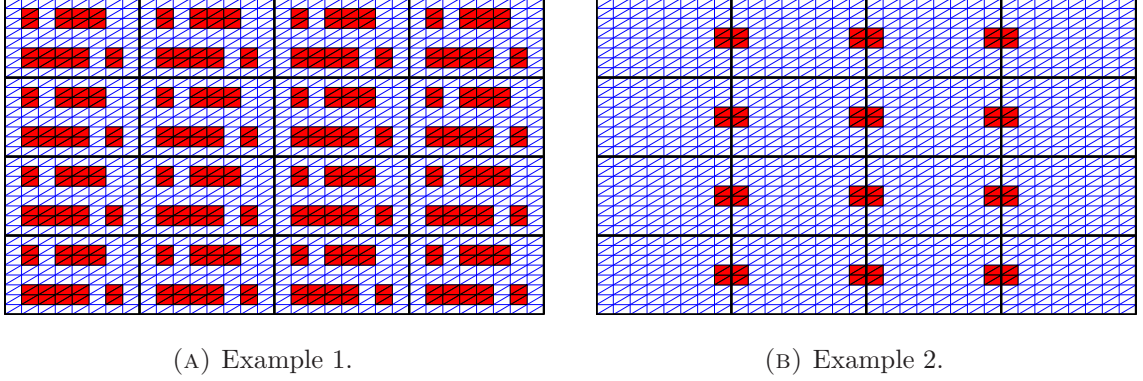


FIGURE 2. Two geometries with 32×32 fine mesh and 4×4 coarse mesh showing the distribution of α . The regions marked with red are where α_1 has a large value.

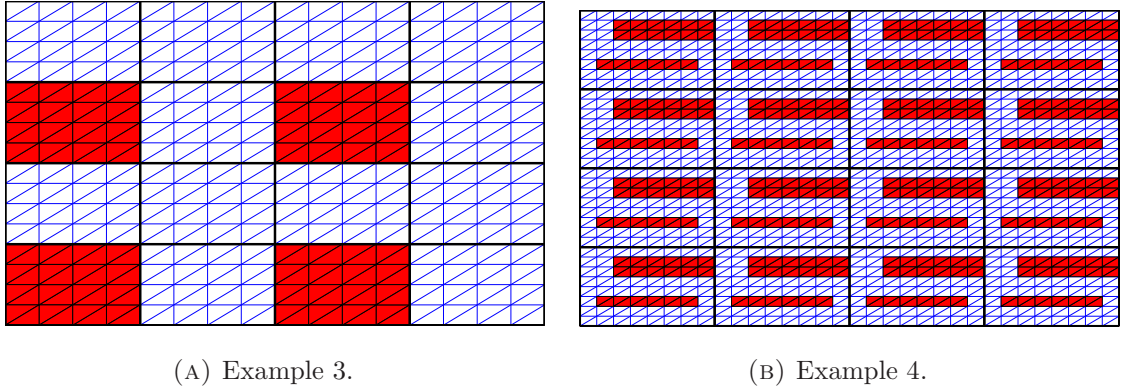


FIGURE 3. (A) Geometry with 16×16 fine mesh and 4×4 coarse mesh showing the distribution of α for the third example. (B) Geometry with 32×32 fine mesh and 4×4 coarse mesh showing the distribution of α for the fourth example. The regions marked with red are where the coefficient has jumps.

The iteration numbers in Table 3 supports our theoretical results developed in Section 4.2. We see no dependency on the contrast in α when the jumps are in the interior of subdomains, cf. Figure 2a. If the coefficient has jumps in the subdomain layer, Ω_i^δ corresponding to Ω_i ,

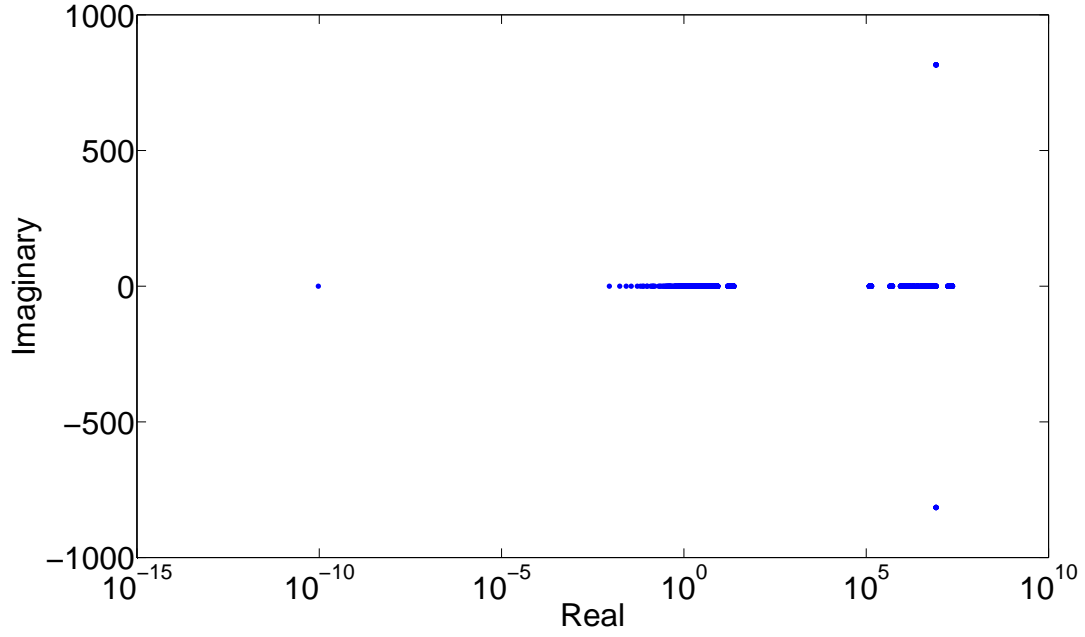


FIGURE 4. Eigenspectrum of the CRFVE stiffness matrix A for the distribution of α given in Example 4 with $\alpha_1 = 1e6$.

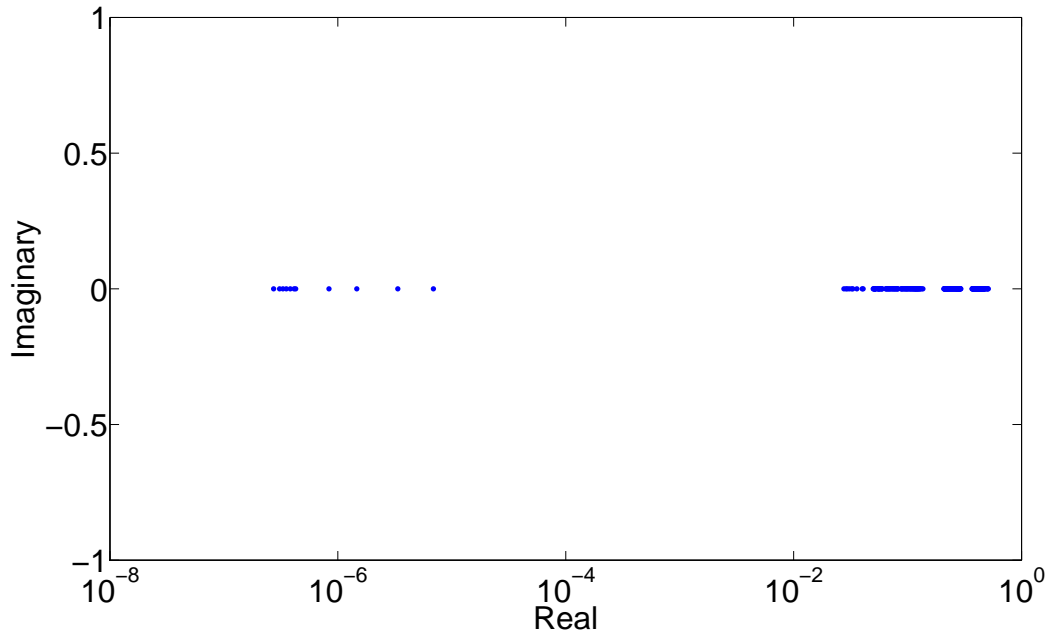


FIGURE 5. Eigenspectrum of the preconditioned operator, $T_A^{(2)}$, for the distribution of α given in Example 4 with $\alpha_1 = 1e6$.

α_1	$\ A - A^t\ _2$	$\ AA^t - A^tA\ _2$
10^0	4.0e-1	6.48e0
10^1	3.96e0	6.03e2
10^2	3.96e1	6.06e4
10^3	3.96e2	6.06e6
10^4	3.96e3	6.06e8
10^5	3.96e4	6.06e10
10^6	3.96e5	6.06e12

TABLE 1. 2-norm measures of the non-symmetry and non-normality of the CRFVE stiffness matrix A with the distribution of α given in Example 4.

h	$\ A^{FE} - A^{FVE}\ _2$ $\alpha = 2 + \sin(100\pi x) \sin(100\pi y)$	$\ A^{FE} - A^{FVE}\ _2$ $\alpha = 2 + \sin(10\pi x) \sin(10\pi y)$	$\ A^{FE} - A^{FVE}\ _2$ $\alpha = 2 + \sin(\pi x) \sin(\pi y)$
1/8	7.16e-1	4.10e0	5.35e-1
1/16	1.02e-1	2.31e0	2.82e-1
1/32	1.52e0	1.16e0	1.44e-1
1/64	4.05e0	6.52e-1	7.28e-2
1/128	3.16e0	3.47e-1	3.65e-2
1/256	1.41e0	1.79e-1	1.84e-2
1/512	7.91e-1	9.09e-2	9.22e-3

TABLE 2. 2-norm measures of the difference between the finite element and the finite volume element stiffness matrix for decreasing h for three different distributions of α .

Average ASM				
	Example 1:	Example 2:	Example 3:	Example 4:
α_1	# iter.	# iter.	# iter.	# iter.
10^0	40	40	31	40
10^1	38	66	32	52
10^2	37	108	36	92
10^3	37	177	36	140
10^4	37	233	38	178
10^5	37	276	39	214
10^6	37	316	39	249

TABLE 3. Number of iterations until convergence for the solution of (1) with different values of α_1 in the distributions of the coefficient α given in Figures 2a, 2b, 3a, 3b.

the method is dependent on the ratio $\frac{\bar{\alpha}_i}{\alpha_i}$, i.e., the ratio of the largest and smallest value of α in the layer, cf. Figure 2b and 3b. When the jumps are only across the substructures,

h/H	1/4	1/8	1/16	1/32	1/64	1/128
1/8	22(1.89e-1)					
1/16	32(8.80e-2)	25(1.67e-1)				
1/32	44(4.22e-2)	37(7.74e-2)	24(1.79e-1)			
1/64	63(2.08e-2)	52(3.78e-2)	35(8.60e-2)	23(1.82e-1)		
1/128	89(1.03e-2)	74(1.87e-2)	49(4.21e-2)	33(8.95e-2)	21(1.83e-1)	
1/256	126(5.12e-3)	106(9.30e-2)	69(2.09e-2)	46(4.42e-2)	29(9.05e-2)	18(1.83e-1)

TABLE 4. Number of iterations for the symmetric preconditioner for decreasing values of h and H with $\alpha = 2 + \sin(10\pi x)\sin(10\pi y)$. Estimates of the smallest eigenvalue of the symmetric part of the preconditioned system are reported in the parentheses.

h/H	1/4	1/8	1/16	1/32	1/64	1/128
1/8	20(1.90e-1)					
1/16	30(9.24e-2)	24(1.79e-1)				
1/32	40(4.54e-2)	33(9.01e-2)	24(1.81e-1)			
1/64	59(2.24e-2)	47(4.45e-2)	35(8.76e-2)	26(1.80e-1)		
1/128	83(1.11e-2)	68(2.19e-2)	49(4.37e-2)	39(8.76e-2)	28(1.70e-1)	
1/256	116(5.50e-3)	95(1.09e-2)	68(2.16e-2)	55(4.29e-2)	41(8.21e-2)	27(1.78e-1)

TABLE 5. Number of iterations for the symmetric preconditioner for decreasing values of h and H with $\alpha = 2 + \sin(100\pi x)\sin(100\pi y)$. Estimates of the smallest eigenvalue of the symmetric part of the preconditioned system are reported in the parentheses.

h/H	1/4	1/8	1/16	1/32	1/64	1/128
1/8	19(1.91e-1)					
1/16	27(9.23e-2)	22(1.83e-1)				
1/32	35(4.54e-2)	32(8.94e-2)	23(1.79e-1)			
1/64	52(2.24e-2)	46(4.40e-2)	35(8.45e-2)	25(1.79e-1)		
1/128	75(1.11e-2)	62(2.20e-2)	46(4.38e-2)	37(8.73e-2)	28(1.70e-1)	
1/256	107(5.50e-3)	89(1.10e-2)	64(2.16e-2)	53(4.28e-2)	40(8.23e-2)	26(1.77e-1)

TABLE 6. Number of iterations for the non-symmetric preconditioner for decreasing values of h and H with $\alpha = 2 + \sin(100\pi x)\sin(100\pi y)$. Estimates of the smallest eigenvalue of the symmetric part of the preconditioned system are reported in the parentheses.

as in Figure 3a, the iteration numbers show that the method is robust with respect to the discontinuities in α .

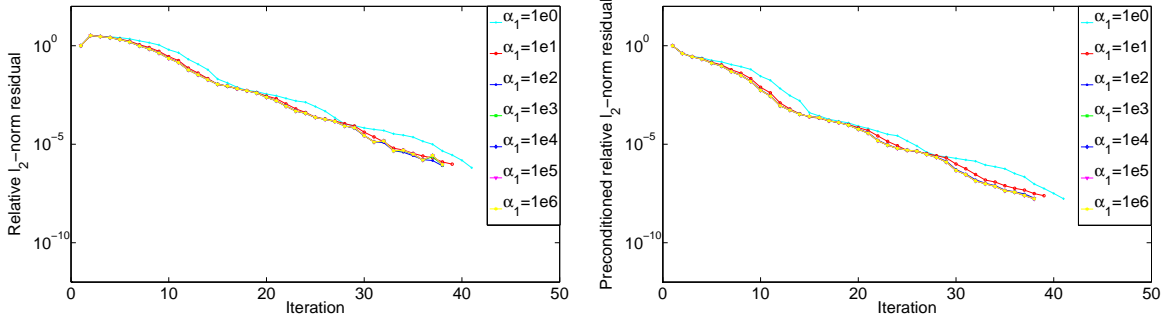
The numerical results also show that the proposed method is asymptotically stable and scalable with respect to the dependence on $\frac{H_i}{h_i}$, and depends linearly on $\frac{H_i}{h_i}$ for the test

cases under consideration as shown in Table 4 and 5. The coefficient α is here equal to $2 + \sin(10\pi x) \sin(10\pi y)$ and $2 + \sin(100\pi x) \sin(100\pi y)$, respectively. By comparing Table 5 and 6, we see that the difference in behavior of the symmetric and non-symmetric preconditioner is negligible.

The distribution of the eigenvalues of the stiffness matrix A , as depicted in Figure 4, include several complex eigenvalues with the magnitude of their complex part being close to zero, and two eigenvalues with multiplicity eight with a clearly visible complex part in the figure. The eigenvalues of the preconditioned operator, as depicted in Figure 5, are all real and positive. Numerical testing have also shown that for the test cases where our theory predicts dependency on the coefficient jump in α , the smallest eigenvalues of the symmetric part of the preconditioned operator, $T_A^{(2)}$, are inversely proportional to the ratio $\frac{\bar{\alpha}_i}{\underline{\alpha}_i}$.

In Figure 6–9 we have plotted the relative residuals and the relative preconditioned residuals measured in the l_2 norm. These plots show that if the stopping criteria is based on the preconditioned residual the method will in the worst case converge to the prescribed tolerance even though the resulting GMRES solution of the linear system is far from the exact solution. Hence, using a stopping criteria based on the l_2 norm of the residual instead of the more commonly used l_2 norm of the preconditioned residual is in our case a much more viable choice.

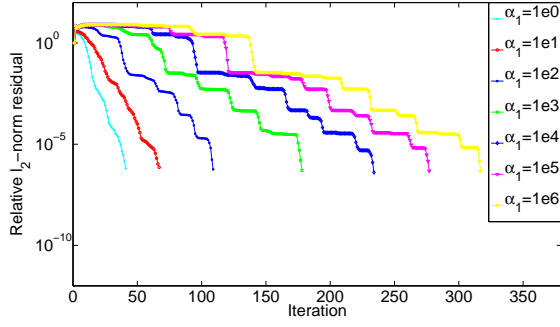
Finally, we conclude this section by stating that the numerical results presented here confirm the theory developed in the previous sections regarding the non-symmetry of the finite volume element stiffness matrix, the estimate for the convergence rate of the GMRES method applied to our preconditioned systems (35) for $k = 2, 3$ and the convergence estimate for the difference between the FE and the FVE bilinear form, cf. Equation (15).



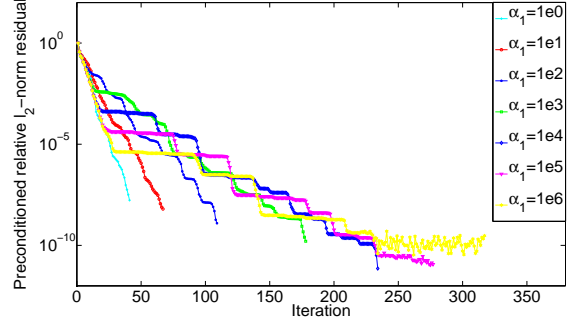
(A) Example 1. Relative residual norms for GMRES minimizing the a -norm for different α_1 .

(B) Example 1. Relative preconditioned residual norms for GMRES minimizing the a -norm for different α_1 .

FIGURE 6

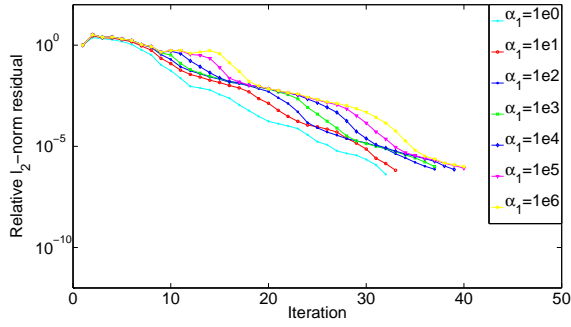


(A) Example 2. Relative residual norms for GMRES minimizing the a -norm for different α_1 .

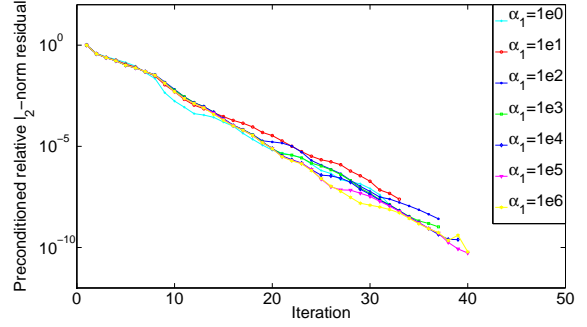


(B) Example 2. Relative preconditioned residual norms for GMRES minimizing the a -norm for different α_1 .

FIGURE 7

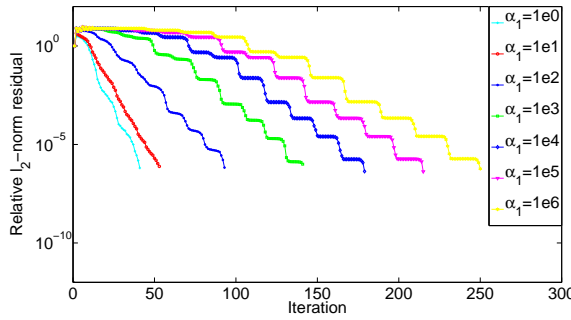


(A) Example 3. Relative residual norms for GMRES minimizing the a -norm for different α_1 .

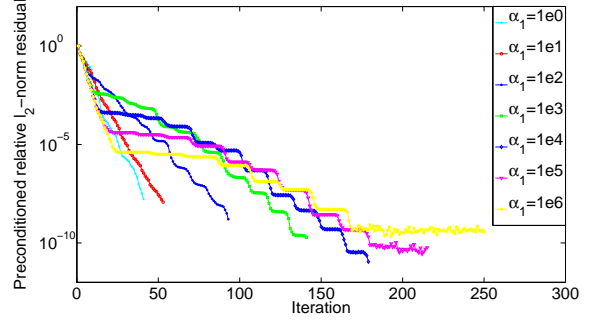


(B) Example 3. Relative preconditioned residual norms for GMRES minimizing the a -norm for different α_1 .

FIGURE 8



(A) Example 4. Relative residual norms for GMRES minimizing the a -norm for different α_1 .



(B) Example 4. Relative preconditioned residual norms for GMRES minimizing the a -norm for different α_1 .

FIGURE 9

REFERENCES

- [1] Randolph E. Bank and Donald J. Rose. Some error estimates for the box method. *SIAM J. Numer. Anal.*, 24(4):777–787, 1987.
- [2] Petter E. Bjørstad, Maksymilian Dryja, and Eero Vainikko. Additive Schwarz methods without subdomain overlap and with new coarse spaces. In *Domain decomposition methods in sciences and engineering (Beijing, 1995)*, pages 141–157. Wiley, Chichester, 1997.
- [3] Susanne C. Brenner. Two-level additive Schwarz preconditioners for nonconforming finite element methods. *Math. Comp.*, 65(215):897–921, 1996.
- [4] Susanne C Brenner and Larkin Ridgway Scott. *The mathematical theory of finite element methods*, volume 15. Springer, 2008.
- [5] Susanne C. Brenner and Li-Yeng Sung. Balancing domain decomposition for nonconforming plate elements. *Numer. Math.*, 83(1):25–52, 1999.
- [6] Xiao-Chuan Cai. *Some domain decomposition algorithms for nonselfadjoint elliptic and parabolic partial differential equations*. ProQuest LLC, Ann Arbor, MI, 1989. Thesis (Ph.D.)–New York University.
- [7] Xiao-Chuan Cai and Olof B. Widlund. Domain decomposition algorithms for indefinite elliptic problems. *SIAM J. Sci. Statist. Comput.*, 13(1):243–258, 1992.
- [8] Zhi Qiang Cai. On the finite volume element method. *Numer. Math.*, 58(7):713–735, 1991.
- [9] Panagiotis Chatzipantelidis. A finite volume method based on the crouzeix–raviart element for elliptic pde’s in two dimensions. *Numerische Mathematik*, 82(3):409–432, 1999.
- [10] Panagiotis Chatzipantelidis. Finite volume methods for elliptic PDE’s: a new approach. *M2AN Math. Model. Numer. Anal.*, 36(2):307–324, 2002.
- [11] SH Chou and J Huang. A domain decomposition algorithm for general covolume methods for elliptic problems. *Journal of Numerical Mathematics jnma*, 11(3):179–194, 2003.
- [12] Victorita Dolean, Frédéric Nataf, Robert Scheichl, and Nicole Spillane. Analysis of a two-level Schwarz method with coarse spaces based on local Dirichlet-to-Neumann maps. *Comput. Methods Appl. Math.*, 12(4):391–414, 2012.
- [13] Maksymilian Dryja and Marcus Sarkis. Additive average schwarz methods for discretization of elliptic problems with highly discontinuous coefficients. *Comput. Methods Appl. Math.*, 10(2):164–176, 2010.
- [14] Stanley C Eisenstat, Howard C Elman, and Martin H Schultz. Variational iterative methods for nonsymmetric systems of linear equations. *SIAM Journal on Numerical Analysis*, 20(2):345–357, 1983.
- [15] R.E. Ewing, T. Lin, and Y. Lin. On the accuracy of the finite volume element method based on piecewise linear polynomials. *SIAM Journal on Numerical Analysis*, pages 1865–1888, 2002.
- [16] Juan Galvis and Yalchin Efendiev. Domain decomposition preconditioners for multiscale flows in high-contrast media. *Multiscale Model. Simul.*, 8(4):1461–1483, 2010.
- [17] Juan Galvis and Yalchin Efendiev. Domain decomposition preconditioners for multiscale flows in high contrast media: reduced dimension coarse spaces. *Multiscale Model. Simul.*, 8(5):1621–1644, 2010.
- [18] I. G. Graham, P. O. Lechner, and R. Scheichl. Domain decomposition for multiscale PDEs. *Numer. Math.*, 106(4):589–626, 2007.
- [19] Wolfgang Hackbusch. On first and second order box schemes. *Computing*, 41(4):277–296, 1989.
- [20] Thomas Y. Hou and Xiao-Hui Wu. A multiscale finite element method for elliptic problems in composite materials and porous media. *J. Comput. Phys.*, 134(1):169–189, 1997.
- [21] Yanping Lin, Jiangguo Liu, and Min Yang. Finite volume element methods: an overview on recent developments. *Int. J. Numer. Anal. Model. Ser. B*, 4(1):14–34, 2013.
- [22] Leszek Marcinkowski. The mortar element method with locally nonconforming elements. *BIT Numerical Mathematics*, 39(4):716–739, 1999.
- [23] Leszek Marcinkowski, Talal Rahman, and Jan Valdman. Additive schwarz preconditioner for the general finite volume element discretization of symmetric elliptic problems. May 2014. Published online in arXiv:1405.0185 [math.NA].
- [24] Talal Rahman, Xuejun Xu, and Ronald Hoppe. Additive schwarz methods for the crouzeix–raviart mortar finite element for elliptic problems with discontinuous coefficients. *Numerische Mathematik*, 101(3):551–572, 2005.
- [25] Hongxing Rui and Chunjia Bi. Convergence analysis of an upwind finite volume element method with crouzeix–raviart element for non-selfadjoint and indefinite problems. *Frontiers of Mathematics in China*, 3(4):563–579, 2008.

- [26] Yousef Saad and Martin H Schultz. Gmres: A generalized minimal residual algorithm for solving nonsymmetric linear systems. *SIAM Journal on scientific and statistical computing*, 7(3):856–869, 1986.
- [27] Marcus Sarkis. Nonstandard coarse spaces and schwarz methods for elliptic problems with discontinuous coefficients using non-conforming elements. *Numerische Mathematik*, 77(3):383–406, 1997.
- [28] Barry Smith, Petter Bjorstad, and William Gropp. *Domain decomposition: parallel multilevel methods for elliptic partial differential equations*. Cambridge University Press, 1996.
- [29] N. Spillane, V. Dolean, P. Hauret, F. Nataf, C. Pechstein, and R. Scheichl. Abstract robust coarse spaces for systems of PDEs via generalized eigenproblems in the overlaps. *Numer. Math.*, 126(4):741–770, 2014.
- [30] Andrea Toselli and Olof B Widlund. *Domain decomposition methods: algorithms and theory*, volume 34. Springer, 2005.
- [31] Haijun Wu and Ronghua Li. Error estimates for finite volume element methods for general second-order elliptic problems. *Numer. Methods Partial Differential Equations*, 19(6):693–708, 2003.
- [32] Sheng Zhang. On domain decomposition algorithms for covolume methods for elliptic problems. *Comput. Methods Appl. Mech. Engrg.*, 196(1-3):24–32, 2006.

DEPARTMENT OF INFORMATICS, UNIVERSITY OF BERGEN, 5020 BERGEN, NORWAY
E-mail address: `Atle.Loneland@ii.uib.no`

FACULTY OF MATHEMATICS, UNIVERSITY OF WARSAW, BANACHA 2, 02-097 WARSZAWA, POLAND.
E-mail address: `Leszek.Marcinkowski@mimuw.edu.pl`

DEPARTMENT OF COMPUTING, MATHEMATICS AND PHYSICS, BERGEN UNIVERSITY COLLEGE, 5020 BERGEN, NORWAY
E-mail address: `Talal.Rahman@hib.no`